Inorganic Chemistry

Article

pubs.acs.org/IC

Bis(toluene)chromium(I) [1,2,5]Thiadiazolo[3,4-*c*][1,2,5]thiadiazolidyl and [1,2,5]Thiadiazolo[3,4-*b*]pyrazinidyl: New Heterospin ($S_1 = S_2 = {}^1/_2$) Radical-Ion Salts

Nikolay A. Semenov,[†] Nikolay A. Pushkarevsky,[‡,§] Elizaveta A. Suturina,[⊥,∥] Elena A. Chulanova,[§,⊥] Natalia V. Kuratieva,[‡] Artem S. Bogomyakov,[¶] Irina G. Irtegova,[†] Nadezhda V. Vasilieva,[†] Lidia S. Konstantinova,[▽] Nina P. Gritsan,*[,⊥,∥] Oleg A. Rakitin,[▽] Victor I. Ovcharenko,[¶] Sergey N. Konchenko,[‡] and Andrey V. Zibarev*[,†,∥]

[†]Institute of Organic Chemistry, [‡]Institute of Inorganic Chemistry, [⊥]Institute of Chemical Kinetics and Combustion, and [¶]International Tomography Center, Siberian Branch of the Russian Academy of Sciences, 630090 Novosibirsk, Russia

[§]Department of Natural Sciences and [∥]Department of Physics, National Research University−Novosibirsk State University, 630090 Novosibirsk, Russia

[▽]Institute of Organic Chemistry, Russian Academy of Sciences, 119991 Moscow, Russia

Supporting Information

ABSTRACT: Bis(toluene)chromium(0), $Cr^0(\eta^6\text{-}C_7H_8)_2$ (**3**), readily reduced [1,2,5]thiadiazolo[3,4-*c*][1,2,5]thiadiazole (**1**) and [1,2,5]thiadiazolo[3,4-*b*]pyrazine (**2**) in a tetrahydrofuran solvent with the formation of heterospin, $S_1 = S_2 = {}^1/_2$, radical-ion salts $[\mathbf{3}]^+[\mathbf{1}]^-$ (**4**) and $[\mathbf{3}]^+[\mathbf{2}]^-$ (**5**) isolated in high yields. The salts **4** and **5** were characterized by single-crystal X-ray diffraction (XRD), solution and solid-state electron paramagnetic resonance, and magnetic susceptibility measurements in the temperature range 2−300 K. Despite the formal similarity of the salts, their crystal structures were very different and, in contrast to **4**, in **5** anions were disordered. For the XRD structures of the salts, parameters of the Heisenberg spin Hamiltonian were calculated using the CASSCF/NEVPT2 and broken-symmetry density functional theory approaches, and the complex magnetic motifs featuring the dominance of antiferromagnetic (AF) interactions were revealed. The experimental χT temperature dependences of the salts were simulated using the Van Vleck formula and a diagonalization of the matrix of the Heisenberg spin Hamiltonian for the clusters of 12 paramagnetic species with periodic boundary conditions. According to the calculations and χT temperature dependence simulation, a simplified magnetic model can be suggested for the salt **4** with AF interactions between the anions ($[\mathbf{1}]^-\cdots[\mathbf{1}]^-$, $J_1 = -5.77$ cm^{-1}) and anions and cations ($[\mathbf{1}]^-\cdots[\mathbf{3}]^+$, $J_2 = -0.84$ cm^{-1}). The magnetic structure of the salt **5** is much more complex and can be characterized by AF interactions between the anions, $[\mathbf{2}]^-\cdots[\mathbf{2}]^-$, and by both AF and ferromagnetic (FM) interactions between the anions and cations, $[\mathbf{2}]^-\cdots[\mathbf{3}]^+$. The contribution from FM interactions to the magnetic properties of the salt **5** is in qualitative agreement with the positive value of the Weiss constant Θ (0.4 K), whereas for salt **4**, the constant is negative (−7.1 K).

INTRODUCTION

Despite rapid progress in the design, synthesis, and structural and functional characterization of molecule-based magnetic and conductive materials for electronics and spintronics, there is a permanent demand for new building blocks in the field.[1] A large number of candidate building blocks came from chalcogen−nitrogen chemistry,[2] especially in the form of neutral and charged π-heterocyclic radicals.[3−8]

Derivatives of the 1,2,5-chalcogenadiazole ring system (Chart 1)[2] can be easily reduced into radical anions (RAs),[8] and the latter can be isolated in the form of thermally stable crystalline salts.[7] The salts, both homospin (where only anions were paramagnetic) and heterospin (where both ions were paramagnetic), revealed antiferromagnetic (AF) interactions in their spin systems.[7]

Chart 1. Archetypal 1,2,5-Chalcogenadiazoles and Their RAs, 1 and 2

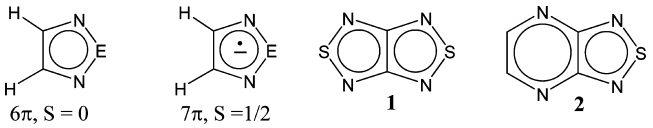

With the McConnell I model[9] dealing with spin polarization, this result is expected for the homospin salts. In these salts, the spin density on the van der Waals (VdW) surfaces of their RAs is mostly positive, with only small islands of negative spin

Received: March 20, 2013
Published: May 21, 2013

   dx.doi.org/10.1021/ic400659q | *Inorg. Chem.* 2013, 52, 6654−6663

density.[10] For neighboring RAs in the crystal lattice, contacts of like spin density are most probable to give rise to AF exchange interactions between them, whereas for ferromagnetic (FM) interactions, contacts of unlike spin density are required[9] [except contacts of unlike density on orthogonal molecular orbitals (MOs) leading to AF interactions].[9a] In principle, such a situation can be achieved with heterospin salts of the discussed RAs, with paramagnetic cations $[MCp_2]^+$ and $[MCp^*_2]^+$ [M = Cr, Mn, Fe; Cp = η^5-C_5H_5; Cp* = η^5-$C_5(CH_3)_5$] possessing peripheral negative spin density on the ligands.[11] However, heterospin, $S_1 = {}^3/_2$ and $S_2 = {}^1/_2$, salt $[CrCp^*_2]^+[\mathbf{1}]^-$ (for **1**, see Chart 1) experimentally revealed only AF effects.[7c] A theoretical study based on the CASSCF and spin-unrestricted broken-symmetry (BS) density functional theory (DFT) calculations led to the conclusion that the magnetic properties of the salt are controlled by its crystal packing, which is favorable for anion−anion and cation−cation AF interactions and unfavorable for anion−cation FM interactions.[7]

For the design and synthesis of magnetic materials, it is important that heterospin systems can also be obtained with neutral radicals when they crystallize in the asymmetric unit containing more than one radical. For such heterospin systems, based on S−N π-heterocyclic radicals, AF and spin-canted AF effects were observed.[3d,e]

It should be noted that currently systems with AF interactions are receiving increased attention because of the experimental observation of the spin-liquid state, as well as their prospects in creating nanoscale memory cells.[12]

According to our calculations (see below), another group of paramagnetic ($S = {}^1/_2$) cations with peripheral negative spin density on ligands consists of $[MAr_2]^+$ (M = Cr, Mo, W). In the chemical context, it is important that (1) the ionization energy (IE) of their precursors MAr_2 (reducing agents in the target salts' preparations)[13] can be varied in a rather broad range depending on the ring substituents (for example, the bigger the number of methyl substituents, the lower the IE) and [14] (2) with the same Ar ligands, the IE is practically equal for M = Cr (3d), Mo (4d), and W (5d) (with Ar = C_6H_6, in 5.40−5.52 eV range),[14] allowing one to cover the whole d block in a single approach. In the physical context, the cations with Mo and W are especially promising because of the strong spin−orbit coupling inherent in these heavy atoms. The strength of the spin−orbit coupling increases sharply with the atomic number as Z^4 to be sufficient for atoms with $Z > 30$. In the heterospin salts containing Mo ($Z = 42$) or W ($Z = 74$) atoms in the cation and heavier chalcogen Se ($Z = 34$) or Te ($Z = 52$) atoms in the anion, the strong spin−orbit coupling can lead to spin canting to originate a FM ground state even under conditions of AF exchange interactions between paramagnetic centers (the Dzyaloshinsky−Moriya mechanism;[9b,15] the spin−orbit contribution to spin-canted AF and FM ordering of Se−N π-heterocyclic radicals was already discussed[3f,g]). An important spectroscopic advantage is that in contrast to the $[CrCp^*_2]^+$ cation, which is undetectable by electron paramagnetic resonance (EPR) spectroscopy because of the fast relaxation and substantial zero-field splitting,[16] $[MAr_2]^+$ (M = Cr, Mo) cations can be detected by conventional EPR techniques.[16,17]

Previously, various $CrAr_2$ were used in the synthesis of radical-ion salts with tetracyanoethylene (TCNE) and 7,7,8,8-tetracyanoquinodimethane (TCNQ). The salts obtained were homospin because only the $[CrAr_2]^+$ cations were paramagnetic ($S = {}^1/_2$), whereas the anions formed diamagnetic ($S = 0$) dimers.[18]

This work begins the application of MAr_2 (M = Cr, Mo, W) compounds to the synthesis of heterospin, $S_1 = {}^1/_2$ and $S_2 = {}^1/_2$, radical-ion salts based on 1,2,5-chalcogenadiazoles and related chalcogen−N π heterocycles. Herein we report on the synthesis and structural and magnetic characterization of two salts obtained by the reduction of [1,2,5]thiadiazolo[3,4-*c*][1,2,5]-thiadiazole and [1,2,5]thiadiazolo[3,4-*b*]pyrazine (**1** and **2**, respectively; Chart 1) with bis(toluene)chromium(0) (**3**) as salts bis(toluene)chromium(I) [1,2,5]thiadiazolo[3,4-*c*][1,2,5]-thiadiazolidyl (**4**) and [1,2,5]thiadiazolo[3,4-*b*]pyrazinidyl (**5**), respectively (Scheme 1).

Scheme 1. Synthesis of 4 and 5

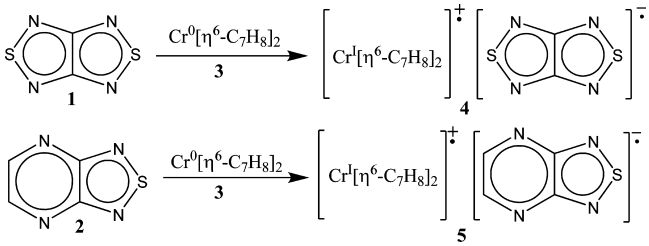

EXPERIMENTAL AND COMPUTATIONAL DETAILS

General Procedure. All operations were carried out under argon using glovebox and Schlenk techniques. Compounds **1** and **2** were prepared by literature methods.[19,20] Compound **3** was synthesized by a known procedure[21] with toluene instead of benzene. Solvents were dried by common methods and distilled under argon.

Cyclic Voltammetry (CV). The CV measurements on degassed 2×10^{-3} M solutions of compound **2** in MeCN were performed at 295 K in an argon atmosphere with a PG 310 USB potentiostat (HEKA Elektronik). The measurements were carried out in a mode of a triangular pulse potential sweep in a three-electrode electrochemical cell ($V = 5$ cm^3) at a stationary platinum electrode ($S = 8$ mm^2), with 0.1 M Et_4NClO_4 as the supporting electrolyte. The sweep rates were 0.01−100 V s^{-1}, and the peak potentials were quoted with reference to a saturated calomel electrode (SCE) used in the measurements as a standard.

EPR Measurements. The solid-state and solution EPR spectra of salts **4** and **5** were recorded on a ELEXSYS-II E500/540 spectrometer (X-band, MW frequency 9.87 GHz, MW power 1 mW, modulation frequency 100 kHz, and modulation amplitude 0.005 mT) equipped with a high-*Q* cylindrical resonator ER4119HS. Numerical simulations of the experimental EPR spectra were performed with the *Winsim 2002* program[22] using the *Simplex* algorithm for optimization of hyperfine coupling (hfc) constants and line widths.

Crystallographic Analysis. The single-crystal X-ray diffraction (XRD) data for compound **2** and salts **4** and **5** (Table 1) were collected with a Bruker DUO APEX diffractometer equipped with a 4K CCD area detector at 150 K with graphite-monochromatized Mo Kα irradiation ($\lambda = 0.71073$ Å). The φ-scan technique was employed to measure intensities. Absorption corrections were applied using the *SADABS* program.[23] The crystal structures were solved by direct methods and refined by full-matrix least-squares techniques with use of the *SHELXTL* package.[24] Atomic thermal parameters for non-H atoms were refined anisotropically. The positions of the H atoms were localized from the difference maps and refined using the riding model. The obtained crystal structures were analyzed for distances between ions by means of the *PLATON* and *MERCURY* programs.[25] The XRD geometries were used in quantum-chemical modeling magnetic properties of the salts.

CCDC 921742 (**2**), CCDC 921740 (**4**), and CCDC 921741 (**5**) contain the supplementary crystallographic data for this paper. These

dx.doi.org/10.1021/ic400659q | Inorg. Chem. 2013, 52, 6654−6663

Table 1. Crystallographic Data for Compounds 2, 4, and 5

	2	4	5
chemical formula	$C_4H_2N_4S$	$C_{16}H_{16}CrN_4S_2$	$C_{18}H_{18}CrN_4S$
fw	138.16	380.45	374.42
T (°C)	−123	−123	−123
λ (Å)	0.71073	0.71073	0.71073
space group	$P2_1/n$ (No. 14)	$C2/c$ (No. 15)	$C2/c$ (No. 15)
a (Å)	11.8139(12)	12.3474(5)	20.2956(7)
b (Å)	3.8646(3)	9.9269(4)	7.2961(2)
c (Å)	23.228(2)	13.0243(5)	14.5246(9)
β (deg)	95.985(2)	105.934(1)	131.325(1)
V (Å^3)	1054.70(17)	1535.07(11)	1615.19(12)
Z, d_{calc} (g cm^{-3})	8, 1.740	4, 1.646	4, 1.540
μ (cm^{-1})	0.499	1.021	0.844
final R indices [$I > 2\sigma(I)$][a]	R1 = 0.0595, wR2 = 0.1632	R1 = 0.0228, wR2 = 0.0656	R1 = 0.0276, wR2 = 0.0752

[a] $R1 = \sum||F_o| - |F_c||/\sum|F_o|$; $wR2 = \{\sum[w(F_o^2 - F_c^2)^2]/\sum[w(F_o^2)^2]\}^{1/2}$.

data can be obtained free of charge from The Cambridge Crystallographic Data Center via www.ccdc.cam.ac.uk/data_request/cif.

Magnetic Measurements and Simulations. The magnetic susceptibility measurements on the salts **4** and **5** were performed with an MPMS-XL Quantum Design SQUID magnetometer in the temperature range 2−300 K in magnetic fields of 500, 1000, 3000, and 5000 Oe. Invariance to the field evidenced the absence of FM impurities in the samples. To calculate the molar magnetic susceptibility (χ) of the salts **4** and **5**, the diamagnetic corrections were estimated using Pascal's constants.[26]

The temperature dependences of χ were simulated using the Van Vleck formula and a diagonalization of the matrix of the Heisenberg spin Hamiltonian for the clusters of 12−16 paramagnetic species.[9b,27] All J values reported herein are based on the phenomenological spin Hamiltonian of the form in eq 1.

$$\hat{H} = -2\sum_{i,j}^{N} J_{ij}\vec{S}_i\vec{S}_j \quad (1)$$

Quantum-Chemical Calculations. Parameters of the Heisenberg spin Hamiltonian (eq 1), viz., the pair exchange coupling constants J_{ij}, were calculated quantum chemically via the energy splitting between the singlet and triplet states of the pairs of paramagnetic species with $S = {}^1/_2$. Earlier, we demonstrated that the exchange parameters J for the pairs of 1,2,5-chalcogenadiazolidyl-type RAs calculated using the spin-unrestricted BS approach[28] at the UB3LYP level of theory[29] are in good agreement with the experiment.[7] In this paper, parameters J were also calculated using the BS approach[28] at the UB3LYP level with the def2-TZVP basis set[30] using the *ORCA* program package.[31] Some estimations were done with the smaller def2-SVP basis set.[32] The J values were calculated according to the formula (2),[33]

$$J = -\frac{(E^{HS} - E^{LS}_{BS})}{\langle S^2\rangle^{HS} - \langle S^2\rangle^{LS}_{BS}} \quad (2)$$

where E^{HS} is the energy of the high-spin state of the pair and E^{LS}_{BS} is the energy of the low-spin state within the BS approach.[28] The accuracy of the energy calculations (self-consistent procedure) was chosen to be 10^{-8} H, which provided values for J with an accuracy of 0.004 cm^{-1}.

Previously for salt $[CrCp^*_2]^+[\mathbf{1}]^-$, for the pairs formed by RAs and cations, the J values calculated using the BS approach were nonrealistically large and the multiconfiguration CASSCF method was employed instead.[7] In this paper, we also were unable to obtain the correct solutions for the BS states of the anion−cation pairs. Thus, the CASSCF and CASSCF/NEVPT2[34] procedures realized in the *ORCA* suit of programs[31] were also employed for calculations of the singlet−triplet splitting ($\Delta E_{ST} = 2J$). In these calculations, the def2-TZVP and smaller def2-SVP bases sets were used.

The ground-state **g** tensor and energies of a series of electronically excited states (doublets and quartets) of the bis(toluene)chromium(I) $[\mathbf{3}]^+$ were calculated at the CASSF/RASSI/SINGLE-ANISO level[35] with the ANO-RCC basis set[36] using the *MOLCAS7.6* suit of programs.[37] Relativistic effects were taken into account based on the Douglas−Kroll Hess Hamiltonian.[38] The active space of the CASSCF calculations (Supporting Information, Figure S1) included nine electrons in nine orbitals: five d atomic orbitals (AOs) of Cr and two π-bonding and two π^*-antibonding MOs of the toluene ligands, which are mixed with d AOs of Cr ($3d^5$ configuration). A total of 1 sextet, 24 quartet, and 75 doublet spin states obtained in the CASSCF calculations were mixed by spin−orbit coupling, giving rise to 252 spin−orbit states using the RASSI module.[35a,b] Finally, the **g** tensor of the lowest Kramers doublet was computed using the SINGLE ANISO module[35c] of the *MOLCAS7.6* program package.[37] The **g** tensors for all paramagnetic species under study were also computed by the B3LYP/DKH method using the EPR/NMR module[39] of the *ORCA* program package.[31]

Syntheses. *Compound 4.* At −30 °C, a solution of 0.177 g (0.75 mmol) of **3** in 5 mL of tetrahydrofuran (THF) was added dropwise for 10 min to a stirred solution of 0.108 g (0.75 mmol) of **1** in 5 mL of THF. The precipitate was filtered off, washed with cold THF, and dried under vacuum. Compound **4** was obtained in the form of dark-red crystals, 0.246 g (86%). Found (calcd for $C_{16}H_{16}CrN_4S_2$): C, 49.9 (50.5); H, 4.3 (4.2); N, 14.3 (14.7); S, 16.5 (16.9). Single crystals suitable for XRD were picked from the bulk of the crystals.

Compound 5. At 0 °C, a solution of 0.095 g (0.40 mmol) of **3** in 5 mL of THF was gradually added for 10 min to a stirred solution of 0.055 g (0.40 mmol) of **2** in 5 mL of THF. The olive-green solution

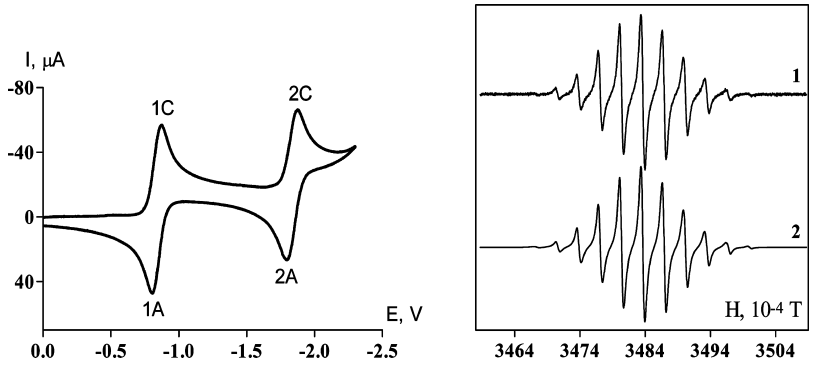

Figure 1. CV of compound **2** at a potential sweep rate of 0.1 V s^{-1} (left) and experimental (1) and simulated (2) EPR spectra of its RA in acetonitrile (right). Experimental (calculated at the UB3LYP/def2-TZVP level) hfc constants (mT): $a_H(H^4,H^5) = 0.338$ (0.302), $a_{N1}(N^2,N^7) = 0.332$ (0.271), $a_{N2}(N^3,N^6) = 0.325$ (0.229); $g = 2.002863$ (2.0055). Previously reported hfc constants (mT) from reduction with elemental K: $a_H(2H) = 0.325$, $a_{N1}(2N) = 0.340$, $a_{N2}(2N) = 0.325$.[8f]

dx.doi.org/10.1021/ic400659q | Inorg. Chem. 2013, 52, 6654−6663

was filtered and slowly evaporated. Compound **5** was obtained in the form of dark needlelike crystals suitable for XRD, 0.140 g (95%). Found (calcd for $C_{18}H_{18}CrN_4S$): C, 57.1 (57.7); H, 4.7 (4.9); N, 14.6 (15.0); S, 8.3 (8.6).

RESULTS AND DISCUSSION

Compounds **1**[7] and **2** (Supporting Information, Figure S2) are 10π-electron heteroaromatics possessing planar molecular structures. They easily form persistent RAs[8f] under conditions of chemical or electrochemical reduction. In MeCN, the electrochemical −1/0 potentials of **1** and **2** vs SCE are −0.59[7] and −0.87 V (Figure 1), respectively. The electrochemically generated RAs of **1**[7] and **2** (Figure 1) are persistent and are characterized by EPR in combination with DFT calculations.

Reduction of heterocycles **1** and **2** with compound **3** (Scheme 1) gave the salts **4** and **5**, respectively, whose structures were confirmed by XRD (Figures 2 and 3). Bis(benzene)chromium(0) reacted similarly; however, single crystals suitable for XRD were not obtained in both cases.

The structure of salt **4** is composed of pillars of alternating cations and RAs, spread along the (1, 0, −1) direction (Figure 2). The anions as well as toluene ligands of the cations are nearly perpendicular to the pillar axis, with their mean planes deflecting by less than 5.2° from the perpendicular plane. Similar moieties in a pillar are symmetrically equivalent, and the distance between the cation (centroid of the toluene C6 ring) and RA (middle of the C−C bond) is 3.53 Å. The centers of the RAs lie on the mean pillar axis, while the cations are shifted to the side of it in an alternating manner (0.67 Å to the Cr atoms). The pillars are stacked in a hexagonal motif across their spreading direction, whereupon the RAs adjoin the cations of four of six adjacent pillars, and vice versa.

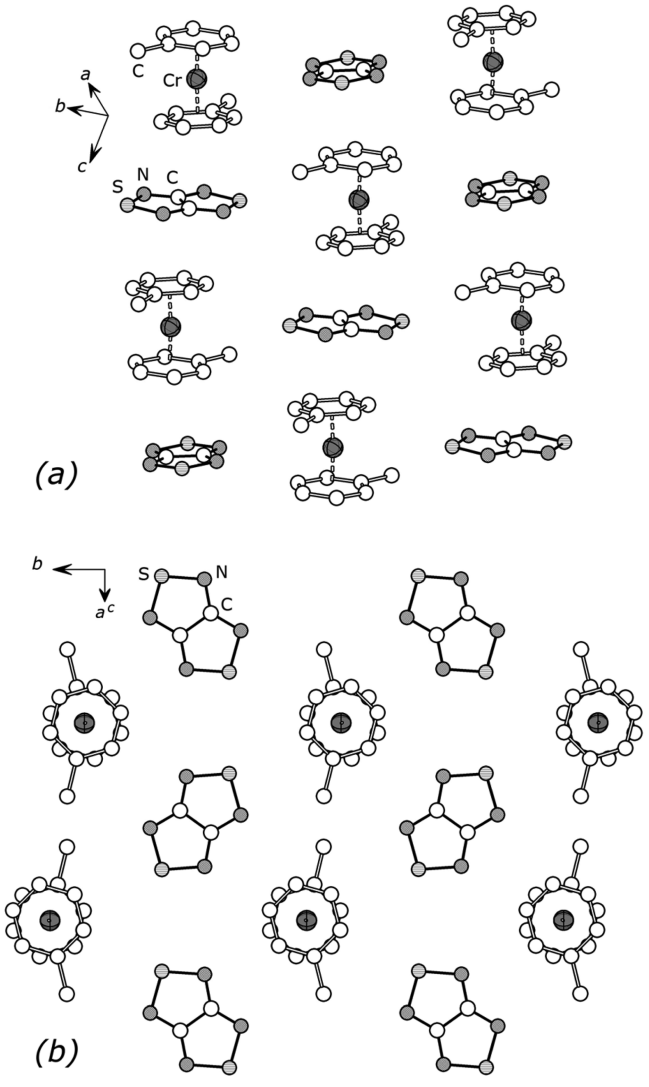

Figure 2. Crystal structure of the salt **4** (H atoms are not shown). Pillars of cations and RAs alternating along the (1, 0, −1) axis (a) and view across the pillar axis (b; only one layer of ions is shown).

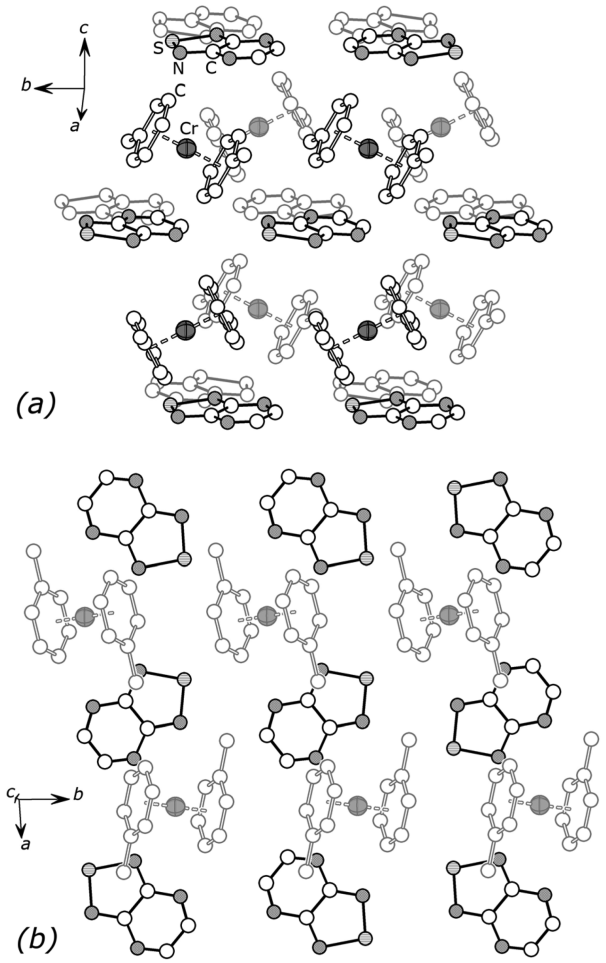

Figure 3. Crystal structure of the salt **5** (H atoms are not shown; disordered RAs are shown in arbitrary directions). Layers of cations and RAs alternating across the *c* axis (a; rear molecules are faded) and view across the layers (b; only one layer of RAs is shown, and foreground cations are faded).

Despite the fact that molecule **2** has nearly the same size and volume as molecule **1**, the stacked motif is absent in the crystal lattice of **5**; instead, the cations and RAs alternate in a layered motif across the *c* axis (Figure 3). The RAs lie close to the mean plane of the layer: individual molecules are inclined by ∼10° off the plane. In contrast, the toluene ligands form an angle of ∼63° with this plane, thus forming a relatively loose cationic layer. The anionic layer is packed in a square-tiled motif, which reminds us that of anion packing in **4**, but unlike the structure of **4**, the cations are out of the plane, approximately over the centers of the squares, formed by four adjacent RAs. The RAs of two adjacent layers are not placed over one another (as in **4**) but taking two alternating positions;

dx.doi.org/10.1021/ic400659q | *Inorg. Chem.* 2013, 52, 6654−6663

the interlayer distance is ~7.26 Å. Hence, the energy of the crystal packing may be less in **5** compared with that in **4**, which is indirectly supported by noticeably better solubility of **5** in organic solvents such as THF and MeCN. The RAs are statistically disordered by the inversion centers located in the center of the middle C−C bond.

Salts **4** and **5** are EPR-active in both the solid state and solution. Solutions in *N*,*N*-dimethylformamide (DMF) and MeCN are stable for several days at ambient temperature, both paramagnetic ions are seen in a 1:1 molar ratio, and the *g*-factor and hfc constants obtained for cation $[\mathbf{3}]^+$ are close to the values measured previously[40] (Figures 4 and 5). In contrast, in

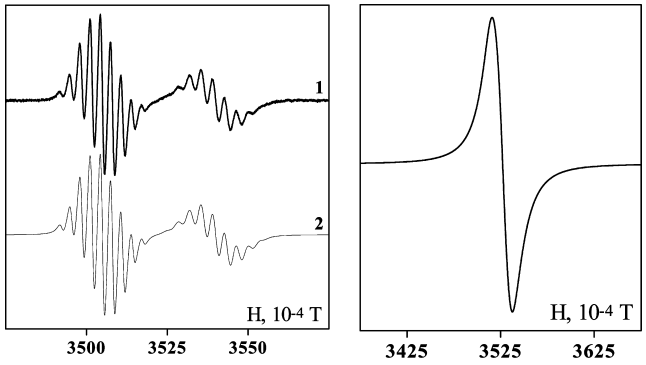

Figure 4. Left: Experimental EPR spectrum of the salt **4** in a DMF solution (1) and its simulation (2). Hfc constants (mT): 0.314 (4N), 0.349 (10H), 0.074 ($2CH_3$). Line widths are 0.137 and 0.150 mT for $[\mathbf{1}]^-$ and $[\mathbf{3}]^+$, respectively, with a $[\mathbf{1}]^-/[\mathbf{3}]^+$ molar ratio of 51:49; g = 2.0093 and 1.9884, respectively. Right: Experimental EPR spectrum in the solid state.

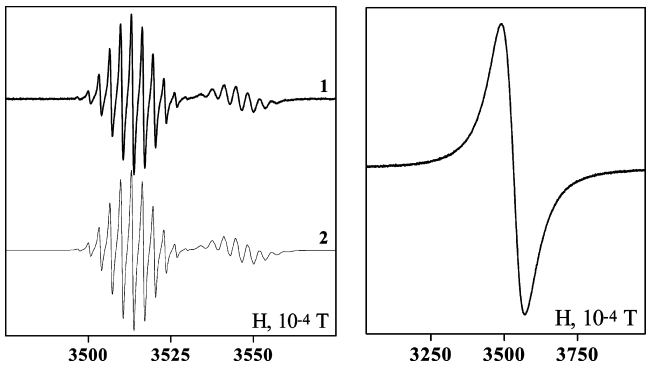

Figure 5. Left: Experimental EPR spectrum of the salt **5** in a DMF solution (1) and its simulation (2). Hfc constants (mT): 0.328 (2N), 0.325 (2N), 0.328 (2H), 0.348 (10H), 0.078 ($2CH_3$). Line widths are 0.067 and 0.094 mT for $[\mathbf{2}]^-$ and $[\mathbf{3}]^+$, respectively, with a $[\mathbf{2}]^-/[\mathbf{3}]^+$ molar ratio of 48:52. Right: Experimental EPR spectrum in the solid state.

better-resolved spectra of the salts' solutions in THF, the intensity of the RA signals decreases relatively fast (Supporting Information, Figure S3), and the salts cannot be recovered from the solutions by precipitation with hexane. The reasons for this are unclear. The solvent-dependent disproportionation, for example, $2[\mathbf{1}]^- \leftrightarrow \mathbf{1} + [\mathbf{1}]^{2-}$, is hardly possible because the equilibrium constant estimated under CV conditions in MeCN is extremely low.[7d]

The EPR spectra of polycrystalline samples of the salts **4** and **5** are broad singlets (Figures 4 and 5).

In the crystal state (Figures 2 and 3), the structures of cation $[\mathbf{3}]^+$ are slightly different, possessing C_2 symmetry in the salt **4** and C_i symmetry in the salt **5** (Figure 6). DFT calculations reproduce fairly well the *g* factors of the RAs and cations: g_{iso} is equal to 2.0073 and 2.0055 for $[\mathbf{1}]^-$ and $[\mathbf{2}]^-$, respectively, and 1.9879 and 1.9883 for the C_2 and C_i structures of $[\mathbf{3}]^+$. g_{iso} = 1.9818 calculated for the C_2 structure of $[\mathbf{3}]^+$ at the CASSCF/RASSI/SINGLE-ANISO level[35] is also in good agreement with the experiment. To calculate this *g* factor, the energies of the ground-state and 99 excited-state multiplets were computed at the CASSCF level. The ground state of $[\mathbf{3}]^+$ is the doublet state, with the main contribution from the configuration with an unpaired electron located at the $3d_{z^2}$ AO (Supporting Information, Figure S1; MO labeled as 3). The two lowest excited doublet states are higher in energy by 10622 and 10999 cm^{-1}. Excitations to these states consist mainly of electron promotion from doubly occupied d_{xy} or $d_{x^2-y^2}$ AOs mixed with π-bonding MOs (Supporting Information, Figure S4; MOs labeled as 2 and 5) to singly occupied d_{z^2} AOs. These low-energy doublets are followed by four quartet states with energies in the range 15870−16520 cm^{-1}.

The spin-density distribution at the VdW surfaces of paramagnetic ions $[\mathbf{1}]^-$, $[\mathbf{2}]^-$, and $[\mathbf{3}]^+$ (with two slightly different geometries) was calculated at the UB3LYP/def2-TZVP level of theory (Figure 6). It is seen that the spin density at the VdW surfaces of RAs is mostly *positive* with an island of *negative* spin density in the vicinity of the C−C bond common for both cycles. The spin density at the VdW surface of cations $[\mathbf{3}]^+$ is close to zero; however, with the cyclic islands of *negative* values in the vicinity of the rings' C atoms. The magnetic properties of the salts are therefore controlled by the way in which these ions are packed in the crystal.

Figure 7 displays the temperature dependences of the molar magnetic susceptibility (χ) for the salts **4** and **5** represented in the form of product χT. The decrease of χT with decreasing temperature indicates the dominance of weak AF interactions between the paramagnetic centers of both salts.

The effective magnetic moments of the salts (μ_{eff}) were calculated using eq 3:

$$\mu_{eff} = \left(\frac{3k}{N\beta^2}\chi T\right)^{1/2} \approx (8\chi T)^{1/2} \quad (3)$$

For both salts at 300 K, μ_{eff} = 2.38 μ_B, which is close to the 2.45 μ_B expected for systems of two noncorrelated spins $S_1 = S_2 = {}^1/_2$ and g = 2. In this case, χT approaches the value of $[g_1^2 S_1(S_1+1) + g_2^2 S_2(S_2+1)]/8 \cong 0.75$ cm^3 K mol^{-1}.

Treatment of the experimental magnetic data in terms of the Curie−Weiss law demonstrated that for both salts the dependence $1/\chi(T)$ obeys the law in the temperature range ~300−50 K and then deviates from linearity (Figure 7). The Curie−Weiss parameters C and Θ are 0.71 cm^3 K mol^{-1} and −7.1 K for **4** and 0.70 cm^3 K mol^{-1} and 0.4 K for **5**, respectively. The values of C are in good agreement with the theoretical spin-only value 0.75 cm^3 K mol^{-1} for both salts **4** and **5**. The positive value of Θ in the case of salt **5** is an indication of the contribution of FM interactions in the spin system of this salt.

To enable an understanding at the molecular level and simulation of the magnetic properties of the salts **4** and **5**, the pair exchange interactions between ions were calculated for the XRD structures (Figures 2 and 3).

dx.doi.org/10.1021/ic400659q | Inorg. Chem. 2013, 52, 6654−6663

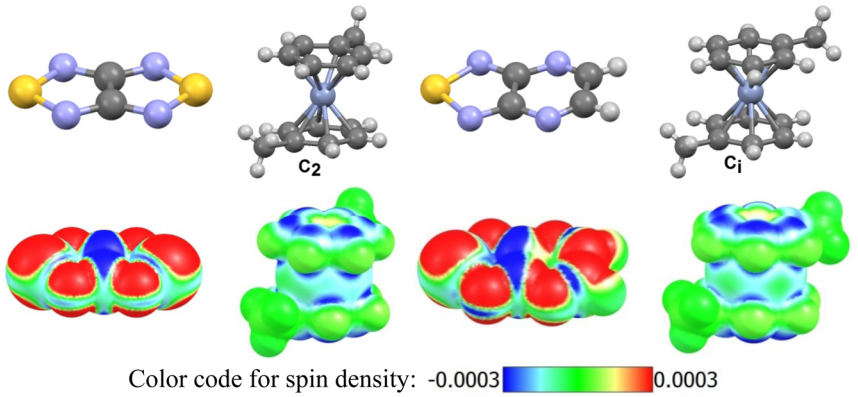

Figure 6. Structures (top; color code: yellow, S; blue, N; gray, C; light blue, Cr; light gray, H) and spin-density distributions at the VdW surfaces (bottom) of the ions of salts **4** (left) and **5** (right) from UB3LYP/def2-TZVP calculations.

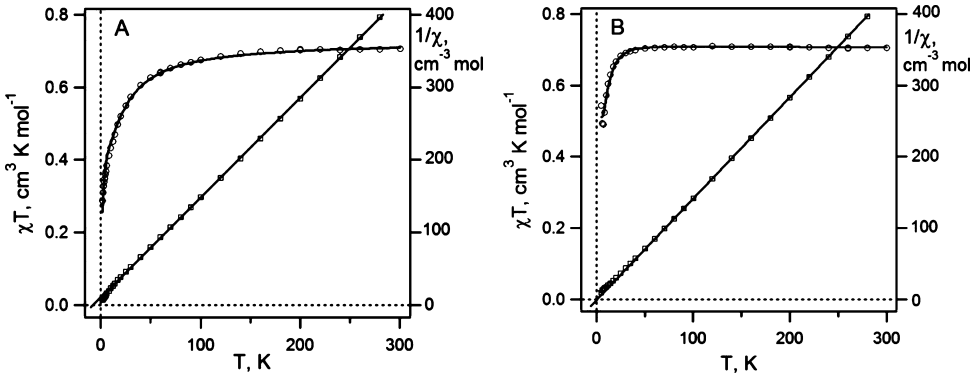

Figure 7. Experimental temperature dependences of χT (○) and $1/\chi$ (□) for the salts **4** (A) and **5** (B) and theoretical approximations of χT (smooth lines) using the Van Vleck equation for a cluster of 12 paramagnetic centers for the salts **4** (Figure 8) and **5** (Figure 9). The best fittings lead to the following parameters: **4**, $J_1 = -5.77$ and $J_2 = -0.84$ cm^{-1}; **5** (oversimplified model consisting of two types of $[\mathbf{2}]^-\cdots[\mathbf{3}]^+$ pairs; see the text), $J_1 = 9.72$ and $J_2 = -7.96$ cm^{-1}. Approximation of the dependences $1/\chi(T)$ (□) of both salts with the Curie–Weiss law (straight lines) is discussed in the text.

In the crystals of **4**, all RAs $[\mathbf{1}]^-$ are structurally equivalent, and every RA has 10 nearest-neighboring RAs. These 10 nearest neighbors give only five unique pairs $[\mathbf{1}]^-\cdots[\mathbf{1}]^-$, with shortest S···S distances in the range 3.98–8.21 Å (Supporting Information, Figure S4). The calculated values of the exchange parameters (J_{ij}) for these pairs are presented in Table 2. According to these data, coupling with nearest neighbors at distances of more than 5 Å can be neglected.

Every cation $[\mathbf{3}]^+$ has six nearest-neighboring RAs, which give only three unique pairs $[\mathbf{1}]^-\cdots[\mathbf{3}]^+$, with shortest Cr···S distances in the range 4.76–5.94 Å (Supporting Information, Figure S5). As mentioned above, we did not obtain correct solutions for BS states of the pairs $[\mathbf{1}]^-\cdots[\mathbf{3}]^+$, and only the results of multiconfiguration calculations are presented in Table 3. The J values for the pairs $[\mathbf{3}]^+\cdots[\mathbf{3}]^+$, with the Cr–Cr distances in the range 7.46–7.92 Å, were calculated at the B3LYP/def2-SVP level and found to be small enough (−0.25 and 0.07 cm^{-1}).

Table 2. Parameters J_{ij} of the $[\mathbf{1}]^-\cdots[\mathbf{1}]^-$ Pair Exchange Interactions Calculated at the UB3LYP, CASSCF, and NEVPT2 Levels of Theory with the def2-TZVP Basis Set

	J, cm^{-1}		
d(S···S),[a] Å	UB3LYP	CASSCF	NEVPT2
3.98	−8.25	−3.70	−7.45
5.22	−1.06	0.25	−0.45
6.93	−0.01	0.00	0.00
7.92	−0.02	0.00	−0.05
8.21	−0.03	0.00	0.00

[a]The shortest S···S distance in the pair (Supporting Information, Figure S4).

Table 3. Parameters J_{ij} of the $[\mathbf{1}]^-\cdots[\mathbf{3}]^+$ Pair Exchange Interactions Calculated at the CASSCF and NEVPT2 Levels of Theory with the def2-TZVP Basis Set

	J, cm^{-1}	
d(S···Cr),[a] Å	CASSCF(2,2)	NEVPT2(2,2)
5.52	1.00	−1.55
4.76	0.25	0.05
5.94	0.05	−0.05

[a]The shortest S···Cr distance in the pair (Supporting Information, Figure S5).

The calculated J values for the pairs $[\mathbf{1}]^-\cdots[\mathbf{1}]^-$ (Table 2) demonstrate that all methods employed here gave qualitatively similar results because they revealed only AF exchange interactions, with one pair being significantly stronger than the others. As previously,[7] the CASSCF calculations predict significantly smaller J values for $[\mathbf{1}]^-\cdots[\mathbf{1}]^-$ pairs than B3LYP calculations. Note that the results of more accurate CASSCF/

dx.doi.org/10.1021/ic400659q | Inorg. Chem. 2013, 52, 6654–6663

NEVPT2 calculations are in good agreement with the DFT data (Table 2).

The CASSCF and NEVPT2 calculations for pairs $[1]^-\cdots[3]^+$ gave qualitatively different results: CASSCF calculations predicted weak FM interactions for all pairs, while more accurate CASSCF/NEVPT2 calculations suggested mainly AF interactions. However, both methods agreed in that the calculated J value for one pair is significantly larger than that for two others. In this pair, the plane of $[1]^-$ is almost parallel to the toluene plane in $[3]^+$ (Supporting Information, Figure S4) and the negative spin density of the toluene ligand is in contact with both the negative spin density in the vicinity of C−C bond and the positive spin density on the N−S−N fragment of $[1]^-$ (Figure 6).

Taking into account the results of the calculations, we proposed the simplified magnetic model for the salt **4** with two nonnegligible J values: J_1 for $[1]^-\cdots[1]^-$ pairs formed by species from neighboring pillars, and J_2 for $[1]^-\cdots[3]^+$ pair formed within the pillars (Figure 8). Simulation of the χT dependence

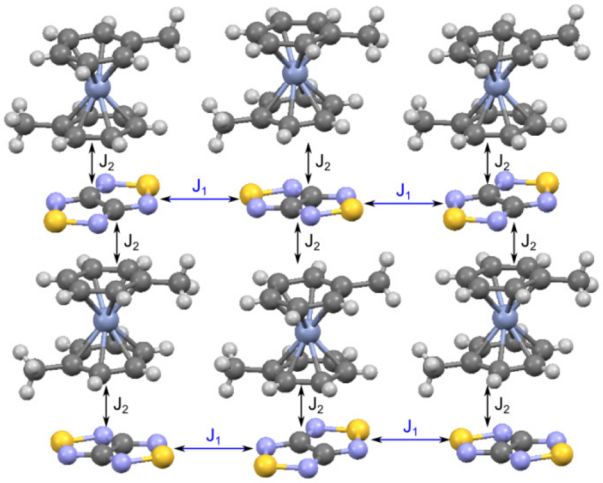

Figure 8. Simplified magnetic model of the salt **4**.

was performed using the Van Vleck formula and a diagonalization of the matrix of Heisenberg spin Hamiltonian (eq 1) for a cluster of 12 paramagnetic species with periodic boundary conditions. The best agreement between theory and experiment was achieved at values $J_1 = -5.77$ and $J_2 = -0.84$ cm^{-1} (Figure 7A). A comparison of these values with the data of Tables 2 and 3 demonstrates that calculations by both the B3LYP and NEVPT2 methods overestimate while the CASSCF method underestimates the exchange interaction between RAs. At the same time, all methods give a reasonable estimate (up to a factor ∼1.5) of the exchange interaction for the $[1]^-\cdots[1]^-$ pair. The agreement between the experimental and NEVPT2-calculated J values for $[1]^-\cdots[3]^+$ pair is also reasonable (−0.84 and −1.55 cm^{-1}, respectively). In turn, the CASSCF calculations predict even the wrong sign of J.

Analysis of the magnetic motif of the salt **5** is much more complicated. One of the complications is the structural disorder of the RAs (Figure 3). For example, every unique $[2]^-\cdots[2]^-$ pair is characterized by three different J parameters, which depend on the mutual orientation of the RAs (Supporting Information, Figure S6). In turn, every cation $[3]^+$ has four neighboring anions $[2]^-$, with the Cr−S distance in the range 5.0−6.6 Å (Supporting Information, Figure S7). Taking into account disorder of the RAs, four different parameters J have to be calculated, and their values are dependent on the spatial orientation of concrete RA in the crystal lattice. The calculated values of the exchange parameters (J_{ij}) for pairs $[2]^-\cdots[2]^-$ and $[2]^-\cdots[3]^+$ are presented in Tables 4 and 5, respectively.

Table 4. Parameters J_{ij} of the $[2]^-\cdots[2]^-$ Pair Exchange Interactions Calculated at the UB3LYP/def2-TZVP, CASSCF/def2-SVP, and NEVPT2/def2-SVP Levels of Theory for Two Unique Pairs in Three Mutual Orientations

		J, cm^{-1}		
d(N···N),[a] Å	mutual orientation	UB3LYP	CASSCF	NEVPT2
3.86	C···C	−0.06	0.30	−0.60
	C···S	−1.76	−0.50	−1.70
	S···S	−3.10	−0.80	−2.20
4.11	C···C	−0.73	0.10	−0.50
	C···S	−0.22	0.00	−0.10
	S···S	−0.37	0.00	−0.20

[a]The shortest N···N distance in the pair (Supporting Information, Figure S6). In this case, the S···S distances cannot be used because the S atoms are distributed over two positions due to disorder.

Table 5. Parameters J_{ij} of the $[2]^-\cdots[3]^+$ Pair Exchange Interactions Calculated at the CASSCF(2,2)/def2-SVP and CASSCF(2,2)/NEVPT2/def2-SVP Levels of Theory

	J, cm^{-1}	
d(S···Cr),[a] Å	CASSCF(2,2)	NEVPT2(2,2)
5.65	2.40	2.50
5.80	−0.60	−2.40
6.11	−2.50	−8.30
6.61	0.90	0.70

[a]The shortest S···Cr distance in the pair (Supporting Information, Figure S7).

Table 4 demonstrates that the B3LYP and CASSCF/NEVPT2 calculations gave qualitatively similar results for pairs $[2]^-\cdots[2]^-$ because they revealed only AF interactions, and for all mutual orientations, the calculated J values for the pair with d(N···N) of 3.86 Å were found to be much larger than that for another one.

In contrast to the J values for the $[2]^-\cdots[2]^-$ pairs, both FM and AF interactions were predicted for the $[2]^-\cdots[3]^+$ pairs (Table 5), with the sign of J dependent on the orientation of $[2]^-$ (Supporting Information, Figure S7). Note that in this case both methods gave qualitatively similar results. The J values for the $[3]^+\cdots[3]^+$ pairs (Supporting Information, Figure S8) were found to be negligible (about −0.1 cm^{-1}).

Overall, one can conclude that the salt **5** has a rather complex 3D magnetic motif. To simulate correctly the χT dependence of the polycrystalline sample of this salt, a diagonalization of the matrix of Heisenberg spin Hamiltonian (eq 1) for a large cluster with at least 36 paramagnetic species should be performed. In addition, the statistical nature of the RA disorder should be taken into account. Unfortunately, this task is intractable, and a cluster with only 12 paramagnetic species was used in our simulations. It was, however, found that with a simplified magnetic model containing seven J parameters (Figure 9) one can obtain very good agreement of the experimental and simulated χT dependences (Figure 7B). The J values featuring both signs were as follows: $J_1 = 7.82$, $J_2 =$

dx.doi.org/10.1021/ic400659q | Inorg. Chem. 2013, 52, 6654−6663

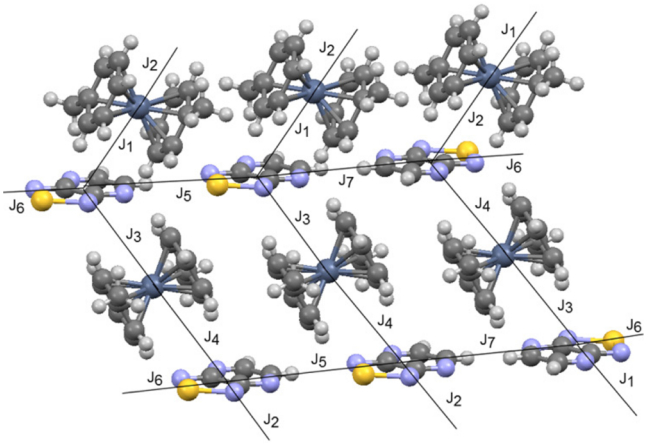

Figure 9. Simplified magnetic model of the salt **5**.

−8.33, J_3 = 2.26, J_4 = 0.52, J_5 = 2.65, J_6 = −0.89, and J_7 = −0.89 cm^{-1}.

The magnetic model shown in Figure 9 is rather complex despite its simplified nature. In any way, it is necessary to account for both FM and AF interactions to reproduce correctly the χT temperature dependence of salt **5**.

To further support the importance of both FM and AF interactions, the χT temperature dependence of salt **5** (Figure 7B) was simulated using the oversimplified model composed of two types of exchange-coupled pairs. In this case, the best fitting led to J_1 = 9.72 and J_2 = −7.96 cm^{-1}, i.e., with account for both FM and AF interactions. This is in qualitative agreement with the results of calculations (Table 3) predicting both types of exchange interactions in the $[\mathbf{2}]^{-}\cdots[\mathbf{3}]^{+}$ pairs. The contribution from the FM interactions is also in qualitative agreement with the positive value of the Weiss constant Θ in the case of salt **5**.

CONCLUSIONS

Under mild conditions, bis(toluene)chromium(0) (**3**) readily reduced **1** and **2** into thermally stable radical-ion salts **4** and **5**. These salts represent a new family of heterospin, $S_1 = S_2 = {}^1/_2$, chalcogen−N π-heterocyclic RA salts. The salts are magnetically active, with dominance of the AF exchange interactions in their spin systems.

The synthetic approach successfully applied in this work to the preparation of new heterospin chalcogen−N π-heterocyclic RA salts may be generalized for a whole d-block because IE is practically equal for MAr_2 compounds (M = Cr, Mo, W) with the same Ar ligands. Target salts with heavy atoms possessing strong spin−orbit coupling, Mo or W atoms in the cations and Se and/or Te atoms in the anions, may satisfy the Dzyaloshinsky−Moriya mechanism for spin canting to originate a FM ground state even under conditions of AF exchange interactions between paramagnetic centers (cf. refs 3f and 3g). Experiments with $MoAr_2$ reducing agents are already in progress.

ASSOCIATED CONTENT

Supporting Information

Orbitals of bis(toluene)chromium(I) involved in the active space for CASSCF calculations, XRD molecular and crystal structure of compound **2**, experimental EPR spectrum of salt **4** along with integral intensities of the anionic and cationic parts, and unique pairs. This material is available free of charge via the Internet at http://pubs.acs.org.

AUTHOR INFORMATION

Corresponding Author

*E-mail: zibarev@nioch.nsc.ru (A.V.Z.), gritsan@kinetics.nsc.ru (N.P.G.).

Notes

The authors declare no competing financial interest.

ACKNOWLEDGMENTS

The authors are grateful to Prof. J. Derek Woollins for valuable discussions and to the Russian Foundation for Basic Research (Projects 10-03-00735, 12-03-31759, and 13-03-00072), the Presidium of the Russian Academy of Sciences (Project 8.14), the Royal Society (RS International Joint Project 2010/R3), the Leverhulme Trust (Project IN-2012-094), and the Siberian Branch of the Russian Academy of Sciences (Project 13) for financial support of various parts of this work. E.A.S. is grateful to the Russian Academy of Sciences for the Golden Medal with Premium for Graduates 2011 and appreciates support from the Ministry for Education and Science of the Russian Federation (Project 14.132.21.1451), the Dynasty Foundation, the Mikhail Prokhorov Foundation, and the International Scientific Charitable Foundation named after K. I. Zamaraev.

REFERENCES

(1) Relevant literature is too abundant to be cited completely. Selected recent references: (a) *Organic Spintronics*; Vardeny, Z. V., Ed.; CRC Press/Taylor & Francis: London, 2010. (b) *Stable Radicals: Fundamentals and Applied Aspects of Odd-Electron Compounds*; Hicks, R. G., Ed.; Wiley: New York, 2010. (c) *Organic Conductors, Superconductors, and Magnets*; Ouahab, L., Yagubskii, E., Eds.; Kluwer: Dordrecht, The Netherlands, 2004. (d) Ratera, I.; Veciana, J. *Chem. Soc. Rev.* **2012**, *41*, 303−349. (e) Wang, C.; Dong, H.; Hu, W.; Liu, Y.; Zhu, D. *Chem. Rev.* **2012**, *112*, 2208−2267. (f) Zhao, Y.; Ling, W. Z. *Chem. Soc. Rev.* **2012**, *41*, 10751087. (g) Figueira-Duarte, T. M.; Muellen, K. *Chem. Rev.* **2011**, *111*, 7260−7314. (h) Anthony, J. E.; Facchetti, A.; Heeney, M.; Marder, S. T. *Adv. Mater.* **2010**, *22*, 3876−3892 (and other acticles of this themed issue). (i) Miller, J. S. *J. Mater. Chem.* **2010**, *20*, 1846−1857. (j) Miller, J. S. *Polyhedron* **2009**, *28*, 1596−1605. (k) Coropceanu, V.; Cornil, J.; Da Silva Filho, D. A.; Olivier, Y.; Silbey, R.; Bredas, J.-L. *Chem. Rev.* **2007**, *107*, 926−952. (l) Bogani, L.; Wernsdorfer, W. *Nat. Mater.* **2008**, 179−186. (m) Saito, G.; Yoshida, Y. *Bull. Chem. Soc. Jpn.* **2007**, *80*, 1−137.

(2) (a) Todres, Z. V. *Chalcogenadiazoles: Chemistry and Applications*; CRC Press/Taylor & Francis: London, 2012. (b) Chivers, T.; Laitinen, R. S. In *Handbook of Chalcogen Chemistry. New Perspectives in Sulfur, Selenium and Tellurium*; Devillanova, F., Ed.; RSC Press: Cambridge, U.K., 2007. (c) Chivers, T. *A Guide to Chalcogen−Nitrogen Chemistry*; World Scientific: Singapore, 2005.

(3) (a) Winter, S. M.; Balo, A. R.; Roberts, R. J.; Lekin, K.; Assoud, A.; Dube, P. A.; Oakley, R. T. *Chem. Commun.* **2013**, *49*, 1603−1605. (b) Lekin, K.; Leitch, A. A.; Tse, J. S.; Bao, X.; Secco, R. A.; Desgreniers, S.; Ohishi, Y.; Oakley, R. T. *Cryst. Growth Des.* **2012**, *12*, 4676−4684. (c) Mailman, A.; Winter, S. M.; Yu, X.; Robertson, C. M.; Yong, W.; Tse, J. S.; Secco, R. A.; Liu, Z.; Dube, P. A.; Howard, J. A. K.; Oakley, R. T. *J. Am. Chem. Soc.* **2012**, *134*, 9886−9889. (d) Yu, X.; Mailman, A.; Lekin, K.; Assoud, A.; Robertson, C. M.; Noll, B. C.; Campana, C. F.; Howard, J. A. K.; Dube, P. A.; Oakley, R. T. *J. Am. Chem. Soc.* **2012**, *134*, 2264−2275. (e) Yu, X.; Mailman, A.; Lekin, K.; Assoud, A.; Dube, P. A.; Oakley, R. T. *Cryst. Growth Des.* **2012**, *12*, 2485−2494. (f) Winter, S. M.; Oakley, R. T.; Kovalev, A. E.; Hill, S. *Phys. Rev. B* **2012**, *85*, 094430. (g) Leitch, A. A.; Brusso, J. L.; Cvrkalj, K.; Reed, R. W.; Robertson, C. M.; Dube, P. A.; Oakley, R. T. *Chem. Commun.* **2007**, 3368−3370 (and other publications of this group).

(4) (a) Haynes, D. A. *Cryst. Eng. Commun.* **2011**, *13*, 4793−4805. (b) Hicks, R. G. In *Stable Radicals: Fundamentals and Applied Aspects of Odd-Electron Compounds*; Hicks, R. G., Ed.; Wiley: New York, 2010. (c) Rawson, J. M.; Alberola, A. In *Handbook of Chalcogen Chemistry. New Perspectives in Sulfur, Selenium and Tellurium*, Devillanova, F., Ed.; RSC Press: Cambridge, U.K., 2007. (d) Awaga, K.; Tanaka, T.; Shirai, T.; Umezono, Y.; Fujita, W. *C. R. Chim.* **2007**, *10*, 52−59. (e) Preuss, K. E. *Dalton Trans.* **2007**, 2357−2369. (f) Awaga, K.; Tanaka, T.; Shirai, T.; Fujimori, M.; Suzuki, Y.; Yoshikava, H.; Fujita, W. *Bull. Chem. Soc. Jpn.* **2006**, *79*, 25−34. (g) Okamoto, K.; Tanaka, T.; Fujita, W.; Awaga, K.; Inabe, T. *Angew. Chem., Int. Ed.* **2006**, *45*, 4516−4518. (h) Fujita, W.; Awaga, K. *Science* **1999**, *286*, 261−262.

(5) (a) Clarke, C. S.; Jornet-Somoza, J.; Mota, F.; Novoa, J. J.; Deumal, M. *J. Am. Chem. Soc.* **2010**, *132*, 17817−17830. (b) Deumal, M.; Rawson, J. M.; Goetha, A. E.; Howard, J. A. K.; Copley, R. C. B.; Robb, M. A.; Novoa, J. J. *Chem.—Eur. J.* **2010**, *16*, 2741−2750. (c) Deumal, M.; LeRoux, S.; Rawson, J. M.; Robb, M. A.; Novoa, J. J. *Polyhedron* **2007**, *26*, 1949−1958. (d) Rawson, J. M.; Alberola, A.; Whalley, A. *J. Mater. Chem.* **2006**, *16*, 2560−2575. (e) Rawson, J.; Luzon, J. M.; Palacio, F. *Coord. Chem. Rev.* **2005**, *249*, 2631−2641.

(6) (a) Shuvaev, K. V.; Passmore, J. *Coord. Chem. Rev.* **2013**, *257*, 1067−1091. (b) Cameron, T. S.; Decken, A.; Grein, F.; Knapp, C.; Passmore, J.; Rautiainen, J. M.; Shuvaev, K. V.; Thompson, R. C.; Wood, D. J. *Inorg. Chem.* **2010**, *49*, 7861−7879 (and previous publications of this group).

(7) (a) Zibarev, A. V.; Mews, R. In *Selenium and Tellurium Chemistry: From Small Molecules to Biomolecules and Materials*; Woollins, J. D., Laitinen, R. S., Eds.; Springer: Berlin, 2011; pp 123−149. (b) Gritsan, N. P.; Zibarev, A. V. *Russ. Chem. Bull.* **2011**, *60*, 2131−2140. (c) Semenov, N. A.; Pushkarevsky, N. A.; Lonchakov, A. V.; Bogomyakov, A. S.; Pritchina, E. A.; Suturina, E. A.; Gritsan, N. P.; Konchenko, S. N.; Mews, R.; Ovcharenko, V. I.; Zibarev, A. V. *Inorg. Chem.* **2010**, *49*, 7558−7564. (d) Makarov, A. Yu.; Irtegova, I. G.; Vasilieva, N. V.; Bagryanskaya, I. Yu.; Borrmann, T.; Gatilov, Yu. V.; Lork, E.; Mews, R.; Stohrer, W.-D.; Zibarev, A. V. *Inorg. Chem.* **2005**, *44*, 7194−7199 (and other publications of this group).

(8) (a) Vasilieva, N. V.; Irtegova, I. G.; Gritsan, N. P.; Lonchakov, A. V.; Makarov, A. Yu.; Shundrin, L. A.; Zibarev, A. V. *J. Phys. Org. Chem.* **2010**, *23*, 536−543. (b) Boere, R. T.; Roemmele, T. L. *Coord. Chem. Rev.* **2000**, *210*, 369−445. (c) Bock, H.; Haenel, P.; Neidlein, R. *Phosphorus Sulfur Relat. Elem.* **1988**, *39*, 235−252. (d) Kaim, W. *J. Organomet. Chem.* **1984**, *264*, 317−326. (e) Hanson, P. *Adv. Heterocycl. Chem.* **1980**, *27*, 31−149. (f) Kwan, C. L.; Carmack, M.; Kochi, J. K. *J. Phys. Chem.* **1976**, *80*, 1786−1792. (g) Kamiya, M.; Akahori, Y. *Bull. Chem. Soc. Jpn.* **1970**, *43*, 268−271. (h) Fajer, J.; Bielski, B. H. J.; Felton, R. H. *J. Phys. Chem.* **1968**, *72*, 1281−1288. (i) Atherton, N. M.; Ockwell, J. N.; Dietz, R. *J. Chem. Soc. A* **1967**, 771−777. (j) Strom, E. T.; Russell, G. A. *J. Am. Chem. Soc.* **1965**, *87*, 3326−3329.

(9) (a) Hirel, C.; Luneau, D.; Pecaut, J.; Öhrström, L.; Bussiere, G.; Reber, C. *Chem.—Eur. J.* **2002**, *8*, 3157−3161. (b) Novoa, J. J.; Deumal, M. *Struct. Bonding (Berlin)* **2001**, *100*, 33−60. (c) Kahn, O. *Molecular Magnetism*; VCH Publishers: New York, 1993. (d) McConnell, H. M. *J. Chem. Phys.* **1963**, *39*, 1910−1917. (e) It is believed the McConnell I mechanism stands behind FM properties of a number of the $[MCp^*_2][X]$ (M = Mn, Fe, Cr; X = TCNE, TCNQ) salts. Miller, J. S. *J. Mater. Chem.* **2010**, *20*, 1846−1857 and references cited therein.

(10) Spin polarization is a consequence of the minimization of electrostatic repulsion of two electrons of parallel spin sharing the same space, according to the Pauli principle. A positive spin density means that the associated magnetic moment is parallel to the net spin moment of the molecule and a negative spin density that the moments are antiparallel. Spin polarization is a real property and can be observed and quantified with polarized neutron diffraction.

(11) (a) Kaupp, M.; Koehler, F. H. *Coord. Chem. Rev.* **2009**, *253*, 2376−2386. (b) Heise, H.; Koehler, F. H.; Herker, M.; Hiller, W. *J. Am. Chem. Soc.* **2002**, *124*, 10823−10832. (c) Kollmar, C.; Kahn, O. *J. Chem. Phys.* **1992**, *96*, 2988−2997.

(12) (a) Han, T.-H.; Helton, J. S.; Chu, S.; Rodriguez-Rivera, J. A.; Broholm, C.; Lee, Y. S. *Nature* **2012**, *492*, 406−410. (b) Loth, S.; Baumann, S.; Lutz, C. P.; Eigler, D. M.; Heinrich, A. J. *Science* **2012**, *335*, 196−198.

(13) Pampaloni, G. *Coord. Chem. Rev.* **2010**, *254*, 402−419. (b) Connelly, N. G.; Geiger, W. E. *Chem. Rev.* **1996**, *96*, 877−910.

(14) (a) Green, J. C. *Struct. Bonding (Berlin)* **1981**, *43*, 37−112. (b) Cloke, F. G. N.; Green, M. L. H.; Morris, G. E. *J. Chem. Soc., Chem. Commun.* **1978**, 72−74. (c) Evans, S.; Green, J. C.; Jackson, S. E. *J. Chem. Soc., Faraday Trans. 2* **1972**, *68*, 249−258. (d) Herberich, G. E.; Mueller, J. *J. Organomet. Chem.* **1969**, *16*, 11−117.

(15) Dzialoshinski, I. *J. Phys. Chem. Solids* **1958**, *4*, 241−255. (b) Moriya, T. *Phys. Rev.* **1960**, *120*, 91−98.

(16) (a) Solodovnikov, S. P. *Russ. Chem. Rev.* **1982**, *51*, 961−974. (b) Warren, K. D. *Struct. Bonding (Berlin)* **1976**, *27*, 45−159.

(17) (a) Calucci, L.; Cloke, F. G. N.; Englert, U.; Hitchcock, P. B.; Pampaloni, G.; Pinzino, C.; Piccini, F.; Volpe, M. *Dalton Trans.* **2006**, 4228−4234. (b) Benetollo, F.; Grigiotti, E.; Laschi, F.; Pampaloni, G.; Volpe, M.; Zanello, P. *J. Solid State Electrochem.* **2005**, *9*, 732−737. (c) Elschenbroich, C.; Moeckel, R.; Zenneck, U.; Clark, D. W. *Ber. Bunsen-Ges.* **1979**, *83*, 1008−1018. (d) Prins, R.; Reinders, F. J. *Chem. Phys. Lett.* **1969**, *3*, 45−48.

(18) (a) Miller, J. S.; O'Hare, D. M.; Chakraborty, A.; Epstein, A. J. *J. Am. Chem. Soc.* **1989**, *111*, 7853−7860. (b) O'Hare, D. M.; Miller, J. S. *Mol. Cryst. Liq. Cryst.* **1989**, *176*, 381−383. (c) Zvarykina, A. V.; Karimov, Yu. S.; Ljubovsky, R. B.; Makova, M. K.; Khidekel, M. L.; Shchegolev, I. F.; Yagubskii, E. B. *Mol. Cryst. Liq. Cryst.* **1970**, *11*, 217−228. (d) Shibaeva, R. P.; Atovmyan, L. O.; Rozenberg, L. P. *J. Chem. Soc., Chem. Commun.* **1969**, 649−650. (e) Shibaeva, R. P.; Atovmyan, L. O.; Orfanova, M. N. *J. Chem. Soc., Chem. Commun.* **1969**, 1494−1495.

(19) Pushkarevsky, N. A.; Lonchakov, A. V.; Semenov, N. A.; Lork, E.; Buravov, L. I.; Konstantinova, L. S.; Silber, T. G.; Robertson, N.; Gritsan, N. P.; Rakitin, O. A.; Woollins, J. D.; Yagubskii, E. B.; Zibarev, A. V. *Synth. Met.* **2012**, *162*, 2267−2276.

(20) Sato, N.; Mizuno, H. *J. Chem. Res. Synop.* **1997**, 250−251.

(21) Fischer, E. O.; Seeholzer, J. *Z. Anorg. Allg. Chem.* **1961**, *312*, 244−263.

(22) Duling, D. R. *J. Magn. Reson. B* **1994**, *104*, 105−110.

(23) *APEX2*, version 2.0; *SAINT*, version 8.18c; *SADABS*, version 2.11; Bruker Advanced X-ray Solutions, Bruker AXS Inc.: Madison, WI, 2000−2012.

(24) Sheldrick, G. M. *Acta Crystallogr.* **2008**, *A64*, 112−122.

(25) (a) Spek, A. L. *PLATON, A Multipurpose Crystallographic Tool*, version 10M; Utrecht University: Utrecht, The Netherlands, 2003. (b) Spek, A. L. *J. Appl. Crystallogr.* **2003**, *36*, 7−13. (c) Macrae, C. F.; Edgington, P. R.; McCabe, P.; Pidcock, E.; Shields, G. P.; Taylor, R.; Towler, J.; van de Stree, M. *J. Appl. Crystallogr.* **2006**, *39*, 453−457.

(26) Kalinnikov, V. T.; Rakitin, Yu. V. *Introduction in Magnetochemistry. Method of Static Magnetic Susceptibility*; Nauka: Moscow, 1980; p 302 (in Russian).

(27) (a) Deumal, M.; Bearpark, M. J.; Novoa, J. J.; Robb, M. A. *J. Phys. Chem. A* **2002**, *106*, 1299−1315. (b) Thompson, L. K.; Waldmann, O.; Xu, Z. *Coord. Chem. Rev.* **2005**, *249*, 2677−2690.

(28) (a) Nagao, H.; Nishino, M.; Shigeta, Y.; Soda, T.; Kitagawa, Y.; Onishi, T.; Yoshika, Y.; Yamaguchi, K. *Coord. Chem. Rev.* **2000**, *198*, 265−295. (b) Noodleman, L.; Case, D. A.; Mouesca, J. M. *Coord. Chem. Rev.* **1995**, *144*, 199−244. (c) Noodleman, L.; Davidson, E. R. *Chem. Phys.* **1986**, *109*, 131−143. (d) Noodleman, L. *J. Chem. Phys.* **1981**, *74*, 5737−5743.

(29) (a) Becke, A. D. *J. Chem. Phys.* **1993**, *98*, 5648−5652. (b) Lee, C.; Yang, W.; Parr, R. G. *Phys. Rev. B* **1988**, *37*, 785−789.

(30) (a) Schaefer, A.; Horn, H.; Ahlrichs, R. *J. Chem. Phys.* **1992**, *97*, 2571−2577. (b) Weigend, F.; Ahlrichs, R. *Phys. Chem. Chem. Phys.* **2005**, *7*, 3297−3305.

(31) Neese, F. *ORCA—An Ab Initio, Density Functional and Semiempirical Program Package*, version 2.8; University of Bonn: Bonn, Germany.

(32) Schaefer, A.; Horn, H.; Ahlrichs, R. *J. Chem. Phys.* **1992**, *97*, 2571−2577.

(33) (a) Soda, T.; Kitagawa, Y.; Onishi, T.; Takano, T.; Shigeta, Y.; Nagao, H.; Yoshioka, Y.; Yamaguchi, K. *Chem. Phys. Lett.* **2000**, *319*, 223−230. (b) Yamaguchi, K.; Takahara, Y.; Fueno, T. In *Applied Quantum Chemistry*; Smith, V. H., Ed.; Reidel: Dordrecht, The Netherlands, 1986; p 155.
(34) (a) Angeli, C.; Cimiraglia, R.; Evangelisti, S.; Leininger, T.; Malrieu, J.-P. *J. Chem. Phys.* **2001**, *114*, 10252−10264. (b) Angeli, C.; Cimiraglia, R.; Malrieu, J.-P. *Chem. Phys. Lett.* **2001**, *350*, 297−305. (c) Angeli, C.; Cimiraglia, R.; Malrieu, J.-P. *J. Chem. Phys.* **2002**, *117*, 9138−9153.
(35) (a) Roos, B. O.; Malmqvist, P.-A. *Phys. Chem. Chem. Phys.* **2004**, *6*, 2919−2927. (b) Malmqvist, P.-A.; Roos, B. O.; Schimmelpfennig, B. *Chem. Phys. Lett.* **2002**, *357*, 230−240. (c) Chibotaru, L. F.; Ungur, L. *J. Chem. Phys.* **2012**, *137*, 064112.
(36) (a) Roos, O.; Lindh, R.; Malmqvist, P.-A.; Veryazov, V.; Widmark, P.-O. *J. Phys. Chem. A* **2005**, *109*, 6575−6579. (b) Roos, B. O.; Lindh, R.; Malmqvist, P.-A.; Veryazov, V.; Widmark, P.-O. *Chem. Phys. Lett.* **2005**, *409*, 295−299.
(37) Aquilante, F.; De Vico, L.; Ferre, N.; Ghigo, G.; Malmqvist, P.-A.; Neogrady, P.; Pedersen, T. B.; Pitoňak, M.; Reiher, M.; Roos, B. O.; Serrano-Andres, L.; Urban, M.; Veryazov, V.; Lindh, R. *J. Comput. Chem.* **2010**, *31*, 224−247.
(38) Hess, B. A.; Marian, C. M.; Wahlgren, U.; Gropen, O. *Chem. Phys. Lett.* **1996**, *251*, 365−371.
(39) Neese, F.; Solomon, E. I. *Inorg. Chem.* **1998**, *37*, 6568−6582.
(40) (a) Gribov, B. G.; Kozyrkin, B. I.; Krivospitskii, A. D.; Chiikin, G. K. *Dokl. Akad. Nauk SSSR* **1970**, *193*, 91−93 (in Russian). (b) Karimov, Y. U.; Chibrikin, V. M.; Shchegolev, I. F. *J. Phys. Chem. Solids* **1963**, *24*, 1683−1687. (c) Anderson, S. E.; Drago, R. S. *J. Am. Chem. Soc.* **1970**, *92*, 4244−4254. (d) Veychinkin, S. I.; Solodovnikov, S. P.; Chibrikin, V. M. *Opt. Spectrom.* **1960**, *8*, 137−142 (in Russian).